

Car Side Window Kinematics

A. Gfrerrer^a, J. Lang^a, A. Harrich^b, M. Hirz^b, J. Mayr^b

^a*Institute of Geometry, Graz University of Technology, Austria*

^b*Institute of Automotive Engineering, Graz University of Technology, Austria*

Abstract

It is a demanding and time-consuming task to construct the side window mechanism of a car such that the deflections along the seals are minimized. The reason for this is that the window surface S delivered by the stylist, will in general not be movable in a proper way: It is required that the surface tightly moves along the seals. Deflections will necessarily occur no matter how much effort the engineer invests. This article describes how to find a spatial motion that minimizes seal deflection for some given automobile side window surface. Necessary but acceptable modification of the stylist's surface S is also addressed, as well as the lifting mechanism design. It is argued that our systematic approach offers considerable savings compared to the prevailing trial-and-error approach.

Keywords: space kinematics, car side window, window lifter mechanism

1. Introduction

Development of modern automotive products and systems is characterized by accelerated production cycles, product diversification and quality enhancement. Use of integrated virtual development methods that combine design, simulation and product management are continually sought. Fig. 1 shows the automotive door development process in the conceptual phase. One major input is the car body styling. The styling data are transferred to the computer aided engineering tools which, in turn, define a door concept by iterative processes.

Email addresses: `gfrerrer@tugraz.at` (A. Gfrerrer), `johann.lang@tugraz.at` (J. Lang), `alexander.harrich@tugraz.at` (A. Harrich), `mario.hirz@tugraz.at` (M. Hirz), `johannes.mayr@tugraz.at` (J. Mayr)

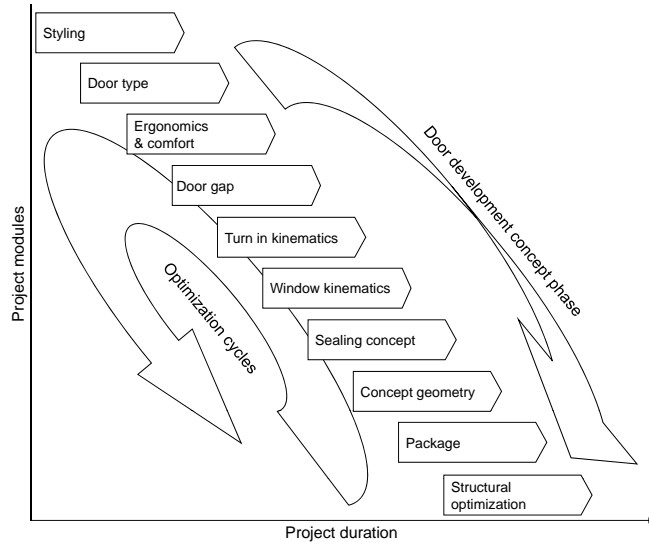


Figure 1: Exemplary automotive door development process in the conceptual phase

Boundary conditions defined by the car styling interact with various engineering-based tasks. Ergonomic studies regarding the entrance area, the seat position and door opening functionalities intimately interact with the outer- (and later on with inner-) shape specifications of the door and its neighboring components. The development of the door gap goes hand in hand with a turn-in analysis and the hinge axis definition. Window kinematics is a challenging door development problem.

Fig. 2 is a symbolic overview of the window kinematics layout process including the main working packages and the data flow. The details of this job are the main part of this paper.

Optimizing the layout of the window kinematics requires computations not supported by commercially available CAD systems. Specific geometry based data are exported into some CAD-external computation software. This includes normals of a given window surface S as well as the B-pillar curve b , the roof curve c and the daylight curve d (see Fig. 3).

The data are used to compute an optimized screw motion M of the given window surface and an additional optimal window surface proposal S_M . Window lifter geometry is developed in a subsequent step. To this end two appropriate anchor points Q, R are specified. The results are reimported to

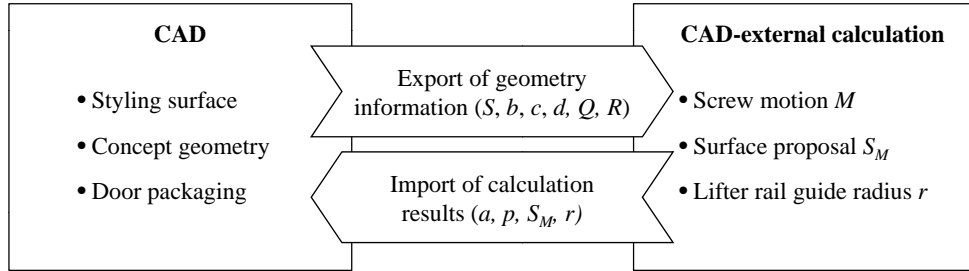


Figure 2: Car side window kinematics layout process

the CAD system and integrated into the conceptual door model to control the corresponding geometries. Within the design process the window kinematics can be evaluated in terms of its feasibility, packaging, function and production.

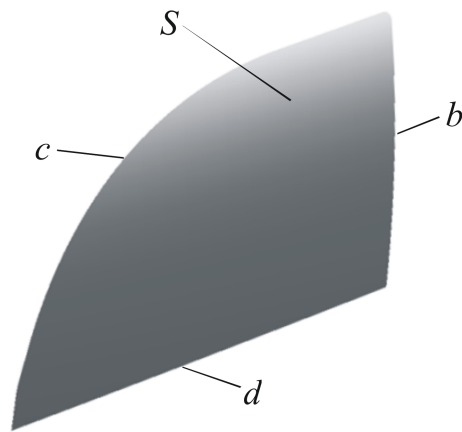


Figure 3: A car side window S and its boundary curves d (daylight curve), b (boundary curve towards the B-pillar) and c (roof curve).

In olden days cars had planar windows. Side windows moved vertically and all points went in straight lines. Today, readily produced, curved car windows contribute to strength, aesthetic and aerodynamic enhancement.

Of course a car window is basically a solid, bounded by a surface (exte-

rior boundary surface) and its offset surface (interior boundary surface) at a certain distance (glass thickness). Additionally it is understood that the window sheet is bounded all around. In the following we consider a surface patch called S representing the exterior boundary of the window pane.

The geometry of a car side window is mainly driven by styling considerations. The proposed window surface S is delivered by the stylist. It is the engineer's job to design an appropriate window lifting mechanism. The main restriction is that the window has to be moved '*in itself*'. Implications of this will be explained in Section 2. It is highly unlikely that a surface S delivered by the stylist incidentally has this property. The engineer's problem is virtually unsolvable. However, small deflections, within limits, are acceptable. It may be possible to find a motion which moves the surface S approximately in itself.

Our approach follows the method suggested in [1], also applied in [2] and [3]. In contrast to [1] we not only consider the given window surface S , but also a curve b which eventually has to become a trajectory of the window motion.

Our method delivers the screw motion M (or in special cases a revolution or a translation) which best fits the given window surface S and the given trajectory b (B-pillar, Section 4). The motion is determined by its screw axis a and its pitch p . The value p in a screw motion is defined as the translatorial distance per turn. With the optimal motion M in mind we can construct a new window surface S_M by subjecting the window roof curve to the motion M . S_M is a screw surface and perfectly moves in itself (Section 2). The given surface S and the surface S_M share the common roof curve. The maximum distance between S and S_M is a measure of the maximum deflection along the seals of S (Section 6). This can be taken as a suitable "figure of merit" of the surface S that was proposed by the stylist. The motion M is the optimal motion to be imposed on the given screw surface S and – at the same time – to S_M . M enables us to construct the optimal window lifter mechanism (inside the door body, Section 7).

2. Moving Curves and Surfaces in Themselves

In this section we explain the concept of '*movability in itself*' for curves and surfaces. From a mathematical standpoint we deal with the invariant curves and surfaces of one-parameter subgroups in the six-parameter Lie-group $SE(3)$ of Euclidean displacements.

It is easy to understand that a straight line g can be moved in itself by a parallel translation right in the direction of g . Such a motion moves any point P on g into another point P' , again on the line g . The whole line remains the same even if no single point on g keeps its position. Thus straight lines are curves which can be moved in themselves. The same holds for circles where the corresponding spatial motion is a revolution about the circle axis. Apart from these two examples there is only one more type of curve to share this property: the helix (Fig. 4). It can be moved in itself by subjecting it to the corresponding screw motion.

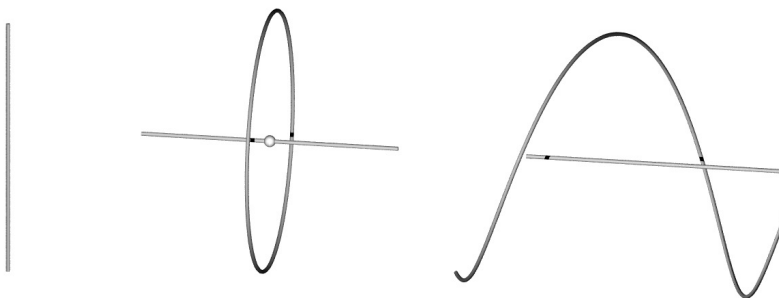


Figure 4: Straight lines, circles and helices are the only curves which can be moved in themselves.

This consideration, albeit theoretical, is applicable to the boundary curve of a side window sheet, e.g. the one towards the B-pillar of a car. But we also have to pose the same question for surfaces:

Which surfaces can be moved in themselves?

The answer is very similar to the answer in the curve case: There are three types belonging to parallel translations, revolutions and screw motions. The types are (Fig. 5)

- cylinder surfaces, generated by a curve being subjected to a parallel translation.
- surfaces of revolution, generated by a curve subjected to a revolution about an axis.
- screw surfaces, generated by a curve subjected to a screw motion.

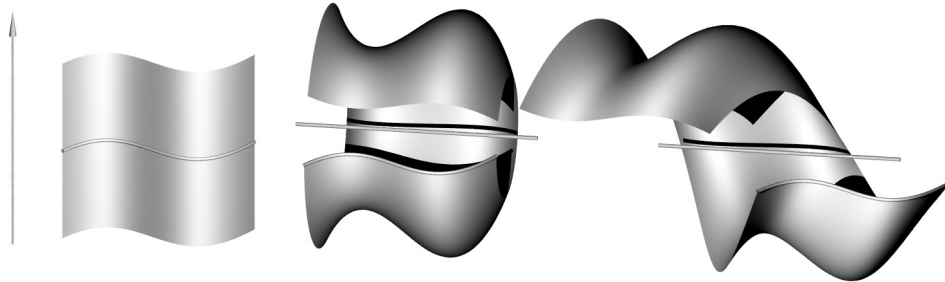


Figure 5: Cylinders, surfaces of revolution and screw surfaces are the only surfaces which can be moved in themselves.

In a way, the first two items can be viewed as special cases of the latter. A rotation is a screw motion where the pitch vanishes, whereas a parallel translation is the limit case of a screw motion where the pitch approaches infinity. In these terms we can state:

Any window sheet moving in itself necessarily is a screw surface.

3. Preliminaries from Line Geometry

In the following we recall some well-known facts from line geometry which we will need further on. For proofs and further details see [4, Chapter 3].

A straight line g in 3-space can be determined by its six ‘*Plücker coordinates*’

$$g_1, g_2, g_3, \bar{g}_1, \bar{g}_2, \bar{g}_3.$$

These six numbers are usually collected in two 3-dimensional vectors

$$\mathbf{g} = \begin{bmatrix} g_1 \\ g_2 \\ g_3 \end{bmatrix}, \quad \bar{\mathbf{g}} = \begin{bmatrix} \bar{g}_1 \\ \bar{g}_2 \\ \bar{g}_3 \end{bmatrix},$$

called ‘*normalized Plücker vectors*’ of g . The term ‘*normalized*’ indicates that the first Plücker vector \mathbf{g} is of norm 1. The Plücker vectors of a line g can be computed as follows: If g is a line with normalized direction vector \mathbf{d} and containing the point P whose position vector is \mathbf{p} then

$$\begin{aligned} \mathbf{g} &= \mathbf{d}, \\ \bar{\mathbf{g}} &= \mathbf{p} \times \mathbf{d}. \end{aligned}$$

Due to this definition the Plücker vectors $\mathbf{g}, \bar{\mathbf{g}}$ of a straight line g have the following properties:

- The components of \mathbf{g} and $\bar{\mathbf{g}}$ always satisfy the homogeneous quadratic equation

$$\mathcal{Q} : \langle \mathbf{g}, \bar{\mathbf{g}} \rangle = g_1 \cdot \bar{g}_1 + g_2 \cdot \bar{g}_2 + g_3 \cdot \bar{g}_3 = 0, \quad (1)$$

called Plücker property. Here $\langle \cdot, \cdot \rangle$ denotes the standard scalar product of two vectors.

- Since $\mathbf{g} = \mathbf{d}$ is a normalized direction vector of g we have

$$\mathcal{Q}^* : \langle \mathbf{g}, \mathbf{g} \rangle = g_1^2 + g_2^2 + g_3^2 = 1. \quad (2)$$

- Replacing the point $P \in g$ by another point $Q \in g$ does not change the second Plücker vector $\bar{\mathbf{g}}$ of g .

By interpreting the Plücker coordinates $g_1, g_2, g_3, \bar{g}_1, \bar{g}_2, \bar{g}_3$ as coordinates of a point G in the six-dimensional space \mathbb{R}^6 we obtain a mapping

$$\kappa : g \longrightarrow G = \kappa(g)$$

from the set of oriented lines in 3-space to a set of points in \mathbb{R}^6 (also compare with [3]). As the coordinates $g_1, g_2, g_3, \bar{g}_1, \bar{g}_2, \bar{g}_3$ have to satisfy (1) and (2) the image points G lie in the intersection \mathcal{G} of the two quadratic surfaces \mathcal{Q} and \mathcal{Q}^* in \mathbb{R}^6 determined by these two equations:

- \mathcal{Q} in Eq. (1) is a quadratic cone whose vertex lies in the coordinate system origin.
- \mathcal{Q}^* in Eq. (2) is a quadratic cylinder with 3-dimensional generator spaces.

The four-dimensional intersection manifold $\mathcal{G} = \mathcal{Q} \cap \mathcal{Q}^*$ is algebraic of degree four.

Conversely, each point $G \in \mathcal{G}$ represents a uniquely determined oriented line g in 3-space as follows:

Let $g_1, g_2, g_3, \bar{g}_1, \bar{g}_2, \bar{g}_3$ be the coordinates of G . After having put $\mathbf{g} := [g_1, g_2, g_3]^\top$, $\bar{\mathbf{g}} := [\bar{g}_1, \bar{g}_2, \bar{g}_3]^\top$ the (normalized) direction vector of the line g is

$$\mathbf{d} = \mathbf{g},$$

whereas

$$\mathbf{p} = \mathbf{g} \times \bar{\mathbf{g}}$$

is the position vector of a point P on g . By the way: P is the pedal point on g w.r.t. the chosen origin.

As a conclusion we have that the mapping κ between the set of oriented lines in 3-space and the set of points on the manifold \mathcal{G} is a bijection.

Let now M denote a screw motion (or, as a special case, a pure rotation or a pure translation). We consider the tangents of the paths generated by M . They establish a vector field which can be written in the form:

$$\dot{\mathbf{p}} = \mathbf{w} \times \mathbf{p} + \mathbf{v}$$

where $\mathbf{v} = [v_1, v_2, v_3]^\top$, $\mathbf{w} = [w_1, w_2, w_3]^\top$ are constant vectors and $\dot{\mathbf{p}}$ denotes the tangent vector of the point P with position vector $\mathbf{p} = [p_1, p_2, p_3]^\top$ (see, for instance [5, p. 25]).

More precisely we have:

- M is a true screw motion if and only if $\mathbf{w} \neq [0, 0, 0]^\top$ and $\langle \mathbf{w}, \mathbf{v} \rangle \neq 0$. In this case

$$p = 2\pi \frac{\langle \mathbf{w}, \mathbf{v} \rangle}{\langle \mathbf{w}, \mathbf{w} \rangle} \quad (3)$$

is the pitch of M ,

$$\mathbf{d} = \mathbf{w} \quad (4)$$

is a direction vector of the screw axis a and

$$\mathbf{a} = \frac{\mathbf{w} \times \mathbf{v}}{\langle \mathbf{w}, \mathbf{w} \rangle} \quad (5)$$

is a position vector of a point $A \in a$.

- M is a rotation if and only if $\mathbf{w} \neq [0, 0, 0]^\top$ but $\langle \mathbf{w}, \mathbf{v} \rangle = 0$. Again the axis of the rotation is determined just as in the screw motion case.
- The motion M is a translation (parallel to \mathbf{v}) if and only if $\mathbf{w} = [0, 0, 0]^\top$.

Let g be a line orthogonal to the path c_P (of a point P) w.r.t. the motion M . Then we obtain

$$\begin{aligned} 0 &= \langle \dot{\mathbf{p}}, \mathbf{g} \rangle = \langle \mathbf{w} \times \mathbf{p} + \mathbf{v}, \mathbf{g} \rangle = \det(\mathbf{w}, \mathbf{p}, \mathbf{g}) + \langle \mathbf{v}, \mathbf{g} \rangle \\ &= \langle \mathbf{w}, \mathbf{p} \times \mathbf{g} \rangle + \langle \mathbf{v}, \mathbf{g} \rangle = \langle \mathbf{w}, \bar{\mathbf{g}} \rangle + \langle \mathbf{v}, \mathbf{g} \rangle, \end{aligned}$$

where $\mathbf{g}, \bar{\mathbf{g}}$ denote the Plücker vectors of g . Thus, the condition

$$\langle \mathbf{v}, \mathbf{g} \rangle + \langle \mathbf{w}, \bar{\mathbf{g}} \rangle = 0 \quad (6)$$

characterizes the set of path normals of the motion M .

Eq. (6) is linear and homogeneous in the Plücker coordinates. Therefore, interpreting this condition in the six-dimensional space \mathbb{R}^6 , we have that the point $G = \kappa(g)$ lies in a hyperplane \mathcal{H}_O passing through the origin O .

The important conclusion is:

If we want to find a screw motion such that a given straight line g belongs to its path normals, we have to look for a hyperplane \mathcal{H}_O of \mathbb{R}^6 through the origin containing the κ -image $G = \kappa(g)$ of g .

Such a hyperplane in \mathbb{R}^6 is determined by 5 points G_1, \dots, G_5 in general position (Fig. 6). Hence, in general we can find exactly one screw motion (including the special cases mentioned above) to a set of five given lines g_1, \dots, g_5 as path normals.

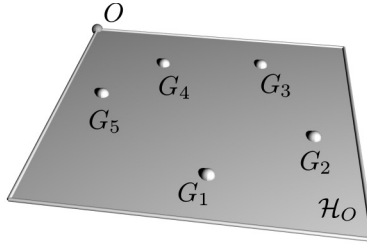


Figure 6: The κ -images G_i and hyperplane \mathcal{H}_O containing them.

Definition: The set of path normals of a screw motion M is called a linear complex. It is denoted by \mathcal{L}_M .

4. Computing the optimal screw motion.

The method which we are following in this section has been suggested in [1] and it has also been applied in [2] and [3]. If a surface S is moved in

itself, any point $P \in S$ follows a path $c_P \subset S$. This implies that the tangent t_P of c_P is orthogonal to the surface normal n_P . We are looking for some screw motion M ; so each surface normal n_P is a path normal of M and thus belongs to the line complex \mathcal{L}_M .

Let us return to the side window matter: In our case we have a set of surface normals $g_i, i = 1, \dots, n$ which are path normals to the screw motion we are determined to find (Fig. 7, left). The κ -images $G_i = \kappa(g_i), i = 1, \dots, n$ of those normals form a ‘point cloud’ (Fig. 7, right). If we are given more than five normals g ($n > 5$) under real-life conditions it is unlikely that the corresponding point cloud lies exactly within one hyperplane \mathcal{H}_O through the origin O . What we can try is finding a hyperplane through O which best fits the point cloud, delivering the least square sum of deviations. This is the core part of the calculation, an optimization process within the 6-dimensional space \mathbb{R}^6 . In the following we describe the single steps of this optimization routine.

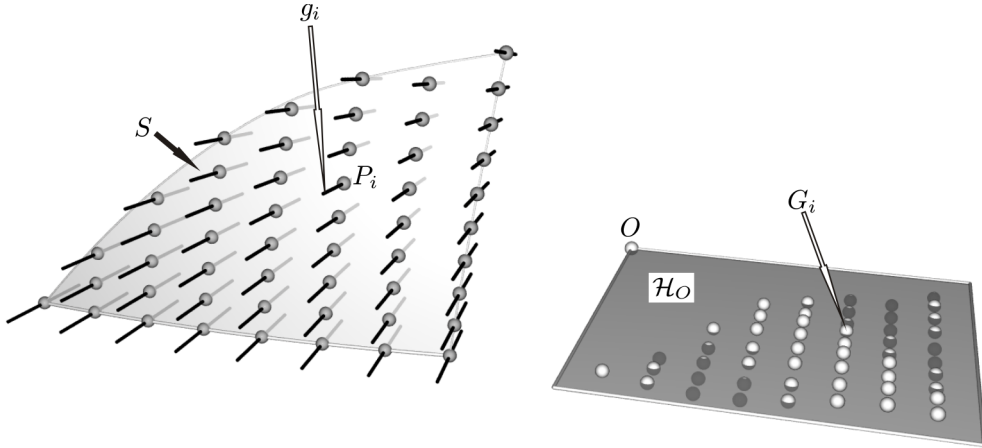


Figure 7: A set of surface normals $\{g_i\}$, the corresponding κ -images $\{G_i\}$ in \mathbb{R}^6 and the optimal hyperplane \mathcal{H}_O .

Let $\mathbf{g}_i, \bar{\mathbf{g}}_i$ be the Plücker vectors of the line g_i . If the points $G_i = \kappa(g_i)$ were indeed within a hyperplane we would have

$$\langle \mathbf{v}, \mathbf{g}_i \rangle + \langle \mathbf{w}, \bar{\mathbf{g}}_i \rangle = 0$$

for $i = 1 \dots n$ with some coefficient vectors \mathbf{v}, \mathbf{w} . For our point cloud this may not be the case.

If $[\mathbf{v}^\top, \mathbf{w}^\top]^\top = [v_1, v_2, v_3, w_1, w_2, w_3]^\top$ denotes the normalized normal vector of the yet unknown hyperplane \mathcal{H}_O , then the squared distance of the point G_i to \mathcal{H}_O is computed via

$$d_i^2 = (\langle \mathbf{v}, \mathbf{g}_i \rangle + \langle \mathbf{w}, \bar{\mathbf{g}}_i \rangle)^2.$$

Hence, we have to minimize the sum

$$f(\mathbf{v}, \mathbf{w}) = \sum_{i=1}^n d_i^2 \quad (7)$$

of squared distances subject to the constraint

$$g(\mathbf{v}, \mathbf{w}) = v_1^2 + v_2^2 + v_3^2 + w_1^2 + w_2^2 + w_3^2 - 1 = 0. \quad (8)$$

The constraint equation guarantees that the normal vector of \mathcal{H}_O has indeed length 1.

Using a Lagrangian multiplier λ for this constraint leads to determining the smallest eigenvalue of a positive semidefinite 6×6 -matrix. For the details the reader is referred to section 2 of [3].

The outcome of the optimization process is called M . In geometrical terms M is a hyperplane through the origin O in the 6-space

$$M \dots \langle \mathbf{v}, \mathbf{g}_i \rangle + \langle \mathbf{w}, \bar{\mathbf{g}}_i \rangle = 0.$$

In mathematical terms we have a 6-vector $[\mathbf{v}^\top, \mathbf{w}^\top]^\top = [v_1, v_2, v_3, w_1, w_2, w_3]^\top$.

5. A prescribed path

The method of [1] will now be modified by additionally considering a given input curve. The motion M we found may be the best possible motion for the given window surface. However, a side window sheet requires one more thing: There is the boundary curve b towards the B-pillar, which is prescribed. It is usually shaped as a seal slit and has to be a path of the window motion M . We obtain additional constraints for the screw motion M to be found.

If each normal to b belongs to the linear complex \mathcal{L}_M we can be sure that b is moved in itself. This implies that b is a path of M , i.e., a helix.

If we are given the boundary curve b it – most probably – is not a helix. We have to find a screw motion with a helical path as close to b as possible. More precisely:

This screw motion M has to fit the window surface S and the B-pillar b at the same time.

The fact that the surface normal in a point $Q \in S$ belongs to the linear complex \mathcal{L}_M signifies the condition that the path of Q is tangent to S in Q . If Q belongs to the curve b we demand even more: The path tangent t_Q to Q is meant to be tangent not only to the window surface S but even to the curve $b \subset S$. All the path normals to b in Q have to belong to the linear complex \mathcal{L}_M . These path normals form a pencil of straight lines (Fig. 8).

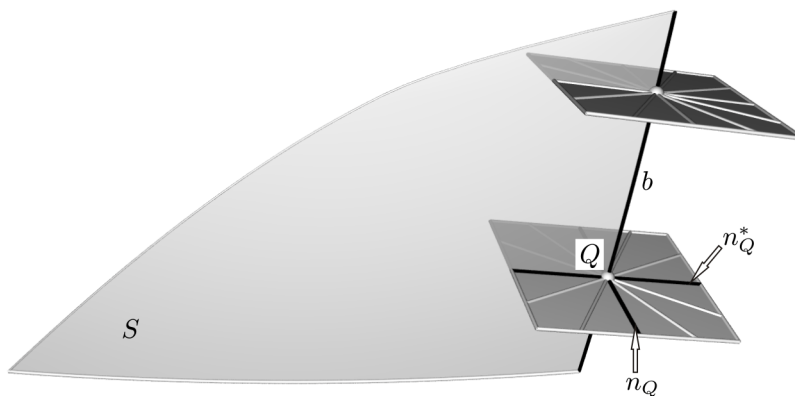


Figure 8: The B-pillar b and its normals.

It is sufficient to pick two lines out of this pencil of lines. Each of these two lines yields a condition which is of the same type as all the other conditions for the surface normals n_P of our window. We can add the surface normal n_Q in Q and one more line. The latter could be the line n_Q^* with the direction orthogonal to both t_Q and n_Q .

If we want to express that our motion M ought to have a trajectory ‘close to the curve b ’ we have to consider several points $Q \in b$ and we have to add a pair of lines for each of them. This adds up to a number of additional lines which have to belong to the linear complex \mathcal{L}_M just as the surface normals. We have a set of further conditions for our optimization problem. The task itself, however, is of the same nature and the algorithm can basically remain unchanged.

Remark: In real life examples we chose 100 surface normals for the window sheet and 50 points along the curve b . Those 50 points Q delivered 50 surface normals n_Q and another 50 lines n_Q^* . So we eventually had 200 straight lines

as the input for our optimization job. The lines yielded 200 points in the 5-space and our method delivered a hyperplane to this point cloud. This hyperplane in turn symbolized a screw motion M .

We have achieved a window motion which fits the B-pillar in terms of moving it in itself and, at the same time, fits the window sheet as perfectly as possible.

Admittedly, there is still the question: How good is ‘*as perfect as possible*’? This question is addressed in the next section.

6. Evaluating the surface

In the past the process of setting up a proper kinematic layout for a side window pane has always been a delicate job. Whatever kinematic solution the engineer brought forward, it was difficult to tell whether the flaws showing up were due to the kinematic mechanism or already inherent in the given window surface design. It is imperative to evaluate the result. To this end we have to find some figure of merit for the outcome.

The screw motion M which we have found moves any screw surface (corresponding to M) perfectly in itself. One such surface which is probably pretty close to the given window sheet, could be constructed in the following way:

We choose a curve c on the given window surface S . This might be any curve e.g., the daylight curve of the window. However, we suggest taking the border curve of S towards the roof together with the border curve towards the A-pillar. We call this joint curve c the ‘*roof curve*’. If we subject this curve c to the optimal screw motion M we create a screw surface S_M .

The surface S_M has the following properties

- S_M moves in itself if the motion M is applied. There is no deflection whatsoever.
- S_M and S share the common roof curve c .

Let m be the maximum distance between S and S_M . This value m is a reliable measure for the maximum deflection caused by the screw motion M if applied to the given window surface S .

The value m can be compared with the deflection limits of the seals manufacturer. This way it is easy to tell whether the kinematic design is within the design target. Just in case that the deflection value m exceeds

the limits, we have a good argument for returning the window sheet design to the stylist. We can even add a suggestion for a perfect replacement S_M with the following appealing properties:

- S_M differs from S by a margin which nowhere exceeds the value m .
- S_M has the same roof curve c as the original proposal S .
- S_M moves perfectly in itself.

If the method is applied at an early stage of the design process this may lead to a perfect solution in the first place.

Remark: For experimental validation we applied the method to an example which is already being produced, and which has already been tried and tested. We arrived at a value m being a fraction of a millimeter. Had our method been applied in the first place it would have surely avoided a lot of cut-and-try.

7. Constructing the lifter mechanism

Fig. 9 shows the configuration of a cable actuated window lifter mechanism with two guides. This type of mechanism has a simple setup and is commonly used in automotive front doors. The sliding blocks moving the window glass are routed along the guide rails. The actuation is performed by an electric motor (formerly by a hand crank) via a Bowden cable driving the capstan.

Once we know the motion M it is easy to devise a suitable mechanism. All we have to do is choose two appropriate anchor points and consider their trajectories. These curves would, theoretically, be perfect guides (rails) for the mechanism. We have to move each of the points on its respective trajectory.

Of course there is always a difference between fundamental considerations and real world applications with their real world constraints. We know the window motion M is a screw motion with axis a and pitch p . A steady screw motion moves every point in space with constant speed. Points with the same speed lie on a right cylinder whose axis coincides with the screw axis a . If there is only one lifter motor it is preferable choose anchor points moving at the same speed to ensure that the lifter cable pulls equally at both rails.

As we know all the details about our screw motion M we can easily see what this constraint brings about: We have to choose two points Q, R

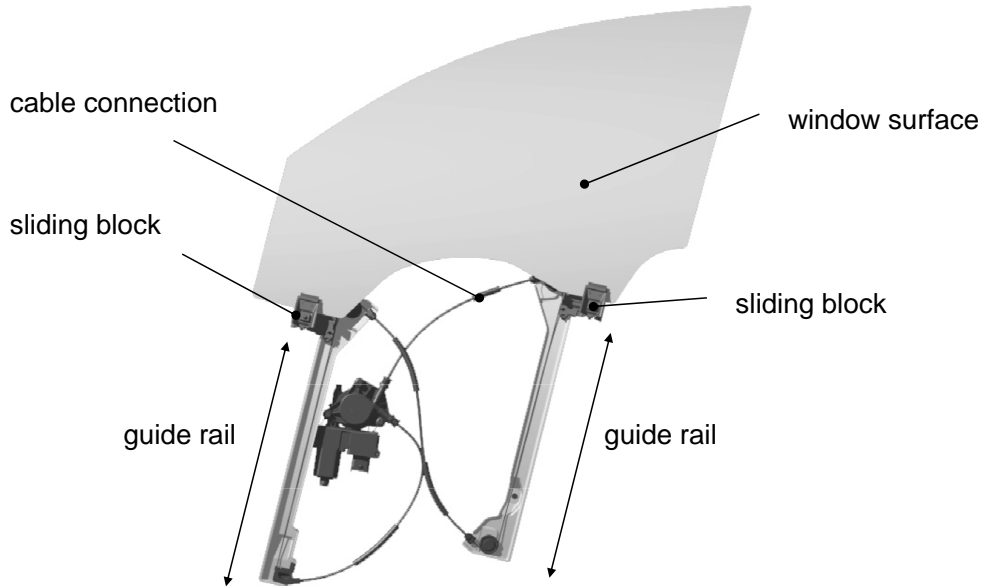


Figure 9: Cable actuated window lifter mechanism with two guides. The dark grey mechanical component between the rails is the electric motor unit.

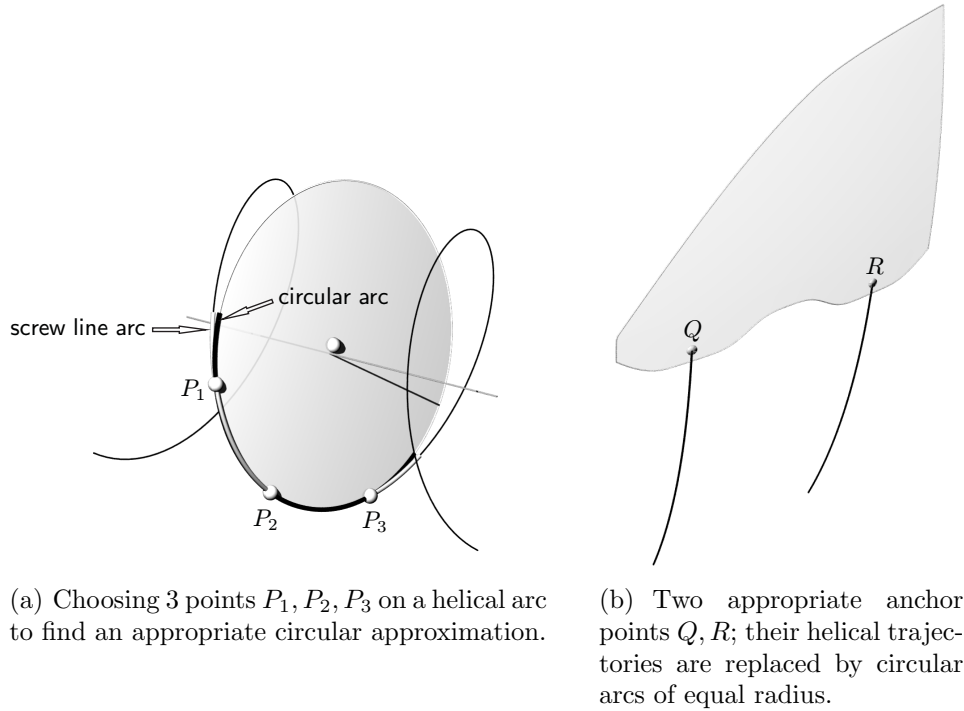
(anchor points, see Section 1) with equal distance from a . They must lie on the same cylinder of revolution with the axis a . Of course the two points have to be located near the bottom boundary curve of the window sheet. After having selected one point the second can still be chosen on the corresponding cylinder surface about a . We merely have to ensure there is no interference within the door cavity.

Screw line rails are spatially curved. Rails in the form of a planar curve are cheaper. The plane curve arc that most closely conforms to a helix is circular. If we replace an optimal helix by an appropriate circle we certainly have to accept some deviation from the ideal motion.

We can easily simulate the effect of replacing the helical rails by circular ones. We choose 3 particular points P_1, P_2, P_3 on the helical arc and construct a circle through these 3 points. Three suitable points are shown in Fig. 10, (a).

In an actual design the helical and circular arcs conform much more closely than those seen in Fig. 10, (a); to emphasize the distinction between the two arcs we intentionally display the helical arc beyond its actually used

range.



(a) Choosing 3 points P_1, P_2, P_3 on a helical arc to find an appropriate circular approximation.

(b) Two appropriate anchor points Q, R ; their helical trajectories are replaced by circular arcs of equal radius.

Figure 10: Replacing the helical arcs by approximating circular segments.

Consider the following specific example with dimensions r (helix radius), p (pitch) and h_W (window height). The values $r = 2000$ mm, $p = 600\pi$ mm and $h_W = 400$ mm deliver¹ a maximum difference between the helical arc and the circular arc of less than 0.05 mm. The two circular rails have the following properties:

- If the two anchor points Q, R (Fig. 10, (b)) are on the same cylinder of revolution about the screw axis a , the two circular arcs have the same radius.
- In this case the point paths along the two rails have the same length. The motion M has the two points move with equal speed on their rails.

¹These figures are approximate but realistic.

- If the two anchor points are even on the same generator of the cylinder of revolution about a and the two circular rails are parallel.

It is not necessary to locate the two anchor points on the same generator (i.e., that they lie on a line parallel to the screw axis a). To have two rails in parallel planes would not bring about any further benefits. It must be pointed out here that the engineers' concern that locating a pair of rails in non-parallel planes would cause the mechanism to stall is unfounded. If the engineer keeps this in mind he or she certainly has one more degree of freedom in designing a lifter mechanism. Considering the confined space within a door body, this may be important.

8. Conclusions

This article has treated the development of side window design from the initially suggested stylist's window surface all the way to the lifter mechanism. The new method was characterized by the fact that we addressed the problem from the bottom up. We worked with the most general set of spatial motions which can move surfaces in themselves. The best motion for any given window surface was derived. Further on we checked the given window and evaluated its quality with respect to the force of friction exerted to the seals. We then constructed a proper mechanism while providing a number of free parameters such that the engineer could allow for spatial restrictions that arise in the preparation of a suitable car door design.

An initial, poorly conceived window surface can be detected and then modified only slightly so as to make it compatible with free movement as well as the stylist's original concept. There will be virtually no deflections along the seals.

Hence, regardless of original window sheet suitability, there are two options. No matter which way we go, we can easily use the optimal screw motion M to construct a suitable window lifter mechanism. Replacing the helical trajectories by circular ones reduces production cost.

In the development stage our approach will contribute considerable savings – and quality improvement – in the development phase of the lengthy and expensive process required to realize a new auto prototype.

The procedure was first outlined at SAE World Congress 2010 in Detroit, USA [6]. Magna Steyr AG has successfully tested and applied our algorithm. We have filed for a patent [7] at Deutsches Patentamt.

References

- [1] H. Pottmann, T. Randrup, Rotational and Helical Surface Approximation for Reverse Engineering, *Computing* 60, 1998, pp. 307–322.
- [2] B. Odehnal, H. Stachel, The upper talocalcanean joint, Technical Report 127, Geometry Preprint Series, Vienna Univ. of Technology, 2004, 12 pages, <http://www.geometrie.tuwien.ac.at/odehnal/knochen.pdf>
- [3] H. Pottmann, M. Hofer, B. Odehnal, J. Wallner, Line Geometry for 3D Shape Understanding and Reconstruction, in: T. Pajdla, J. Matas (Eds.), *Computer Vision – ECCV 2004*, Part I, Vol. 3021 of Lecture Notes in Computer Science, 1999, pp. 297–309.
- [4] H. Pottmann, J. Wallner, *Computational Line Geometry*, Springer, 2000.
- [5] O. Bottema, B. Roth, *Theoretical Kinematics*, Dover Publications, 1990.
- [6] A. Harrich, J. Mayr, M. Hirz, P. Rossbacher, J. Lang, A. Gfrerrer, A. Haselwanter, CAD-based synthesis of a window lifter mechanism, in: *SAE World Congress*, 2010, Detroit, USA.
- [7] A. Gfrerrer, J. Lang, M. Hirz, A. Harrich, J. Mayr, A. Haselwanter, G. Bindar, Verfahren und Vorrichtung zum Ermitteln einer Sollbewegung, zum Bewegen und zum Modifizieren eines verfahrbaren Bauteils, pat. pend. DE10 2010 003 882.2, 12.04.2010, Deutsches Patentamt.

Authors biographies

Anton Gferrer received the M.S. degree in mathematics and descriptive geometry from the University of Graz, Graz, Austria, in 1989 and the Ph.D. degree from Graz University of Technology (TU Graz) in 1992. He is currently an Associate Professor with the Institute for Geometry, TU Graz, and also teaches at the University of Leoben. His research fields are geometry, kinematics and robotics.

Johann Lang received his M.S. degree in mathematics and descriptive geometry at Graz University in 1977 and his Ph.D. degree at Graz University of Technology (TU Graz) in 1979. He is currently an Associate Professor with the Institute for Geometry, TU Graz. His research fields are geometry and kinematics.

Alexander Harrich was born 1982 in Klagenfurt, Austria.

Education: 2005 Master's Degree in Automotive Engineering at University of Applied Sciences FH Joanneum, Graz
Job history: Since 2005 Scientific researcher at Graz University of Technology, Institute of Automotive Engineering. Research projects in the area of dynamic brake- and suspension testing (2005 - 2008). Since 2008: Doctoral student at the Institute of Automotive Engineering. Research field: Advanced design methods.

Mario Hirz was born 1973 in Austria.

Education: Master study of mechanical engineering and economic science at Graz University of Technology. Doctoral study at the Institute of Internal Combustion Engines and Thermodynamics.

Job history: Between 2000 and 2007: Vice head of the Section Design at the Institute of Internal Combustion Engines and Thermodynamics. Since 2007: Research assistant at the Institute of Automotive Engineering. Project manager of several international engine- and vehicle research projects. Lecturer at Universities and in the automotive industry in Europe and Asia. Research activities in the area of virtual product development. About 90 publications, several national and international awards.

Johannes Mayr was born 1984 in Graz, Austria.

Education: Study of Mechanical Engineering and Economics, Graz University of Technology

Job history: From 2005 to 2008 design engineer in the automotive industry at Magna Engineering Center. International experience in projects in Great Britain and Saudi Arabia. Since 2008 research assistant at the Institute of Automotive Engineering at Graz University of Technology. Research activities in the area of 3D-CAD and development methods.